Acta Crystallographica Section F
Structural Biology and Crystallization Communications
ISSN 1744-3091

Preliminary crystallographic analysis of the major capsid protein P2 of the lipid-containing bacteriophage PM2

Nicola G. A. Abrescia,[a] Hanna M. Kivelä,[b] Jonathan M. Grimes,[a] Jaana K. H. Bamford,[b] Dennis H. Bamford[b] and David I. Stuart[a]*

[a]Division of Structural Biology, The Wellcome Trust Centre for Human Genetics, University of Oxford, Roosevelt Drive, Headington, Oxford OX3 7BN, England, and [b]Institute of Biotechnology and Department of Biological and Environmental Sciences, University of Helsinki, PO Box 56, Viikinkaari 5, 00014 University of Helsinki, Finland

Correspondence e-mail: dave@strubi.ox.ac.uk

Received 6 April 2005
Accepted 5 July 2005
Online 30 July 2005

PM2 (*Corticoviridae*) is a dsDNA bacteriophage which contains a lipid membrane beneath its icosahedral capsid. In this respect it resembles bacteriophage PRD1 (*Tectiviridae*), although it is not known whether the similarity extends to the detailed molecular architecture of the virus, for instance the fold of the major coat protein P2. Structural analysis of PM2 has been initiated and virus-derived P2 has been crystallized by sitting-nanodrop vapour diffusion. Crystals of P2 have been obtained in space group $P2_12_12$, with two trimers in the asymmetric unit and unit-cell parameters a = 171.1, b = 78.7, c = 130.1 Å. The crystals diffract to 4 Å resolution at the ESRF BM14 beamline (Grenoble, France) and the orientation of the non-crystallographic threefold axes, the spatial relationship between the two trimers and the packing of the trimers within the unit cell have been determined. The trimers form tightly packed layers consistent with the crystal morphology, possibly recapitulating aspects of the arrangement of subunits in the virus.

1. Introduction

Corticoviruses, of which PM2 is the only representative to date, have similarities to *Tectiviruses* (type-species bacteriophage PRD1; Abrescia *et al.*, 2004; Cockburn *et al.*, 2004) in terms of capsid size and the presence of lipids (ICTVdB – The Universal Virus Database v.3; Büchen-Osmond, 2003). PM2 is a bacterial parasite belonging to the marine virus community and was isolated from the seawater off the coast of Viña del Mar in Chile. It was the first lipid-containing bacteriophage to be characterized (Espejo & Canelo, 1968*a*) and infects two *Pseudoalteromonas* species (Espejo & Canelo, 1968*b*; Kivelä *et al.*, 1999). PM2 has a circular highly (negatively) supercoiled double-stranded DNA genome (10 079 bp) enclosed in a lipid vesicle that is in turn surrounded by an icosahedral capsid shell (Harrison *et al.*, 1971; Huiskonen *et al.*, 2004; Männistö *et al.*, 1999). The virion is composed of at least ten structural proteins. Two of them, P1 (37.5 kDa) and P2 (30.2 kDa), constitute the pentameric spike vertex and the major protein of the capsid shell, respectively; the remaining eight proteins P3, P4, P5, P6, P7, P8, P9 and P10 are membrane-associated (Kivelä *et al.*, 2002; Huiskonen *et al.*, 2004). None of these viral proteins have been crystallized in isolation.

Cryo-EM analysis (Huiskonen *et al.*, 2004) and X-ray studies (Abrescia *et al.*, unpublished results) of the entire PM2 bacteriophage show 600 monomers of the major capsid protein P2 arranged on a pseudo-T = 21 lattice. P2 shows a pseudo-hexameric morphology and biochemical data suggest that it is trimeric (Kivelä *et al.*, 2002); however, no structural information is available on its fold. The double-β-barrel trimeric fold adopted by the major capsid proteins of several large icosahedral viruses has been proposed to indicate common ancestry (Bamford *et al.*, 2002; Nandhagopal *et al.*, 2002; Benson *et al.*, 2004). This view of viral lineages based on a set of viral core properties, such as the coat-protein fold and assembly principles, that are conserved through evolution provides a simplifying principle for virus taxonomy (Bamford, 2003).

In order to better understand the architecture of PM2, its evolutionary relationship with PRD1 (Benson *et al.*, 2004), virus-assembly mechanisms and the potential role of the lipids in virus morphogenesis, we have (in the absence of crystals of the intact virus that diffract to high resolution) initiated a *divide et impera* approach to the

structural analysis of the PM2 bacteriophage. Here, we describe the crystallization of the major capsid protein P2, confirm its trimeric state by self-rotation function analysis and reveal the organization of the trimers into layers within the crystal.

2. Material and methods

2.1. Protein P2 isolation and purification

Protein P2 was purified from disrupted PM2 virus particles. Bacteriophage and host bacterium *Pseudoalteromonas* sp. ER72M2 were cultured in SB medium (Kivelä *et al.*, 1999). Virus particles were purified as previously described using rate zonal sucrose ultracentrifugation, except that the purification buffer was 20 m*M* MOPS pH 7.4, 100 m*M* NaCl, 5 m*M* $CaCl_2$ (Kivelä *et al.*, 1999). Concentrated viruses (∼2.5 mg ml^{-1} protein) were dissociated by addition of EGTA (to a final concentration of 50 m*M*) and by three cycles of freezing (253 K) and thawing. After centrifugation (Beckman Ti-50 rotor, 40 000 rev min^{-1}, 1 h, 277 K), the supernatant containing P2 was dialyzed against 20 m*M* Tris–HCl pH 7.2 containing 30 m*M* NaCl (16 h, 277 K) and loaded onto an anion-exchange column [HiTrap Q Sepharose (Amersham Pharmacia Biotech) equilibrated with 20 m*M* Tris–HCl pH 7.2, 30 m*M* NaCl at 295 K]. The flowthrough containing P2 was further purified by size-exclusion chromatography [Superdex 200, 26/60 (Amersham Pharmacia Biotech) equilibrated with 20 m*M* Tris–HCl pH 7.2, 150 m*M* NaCl at 295 K].

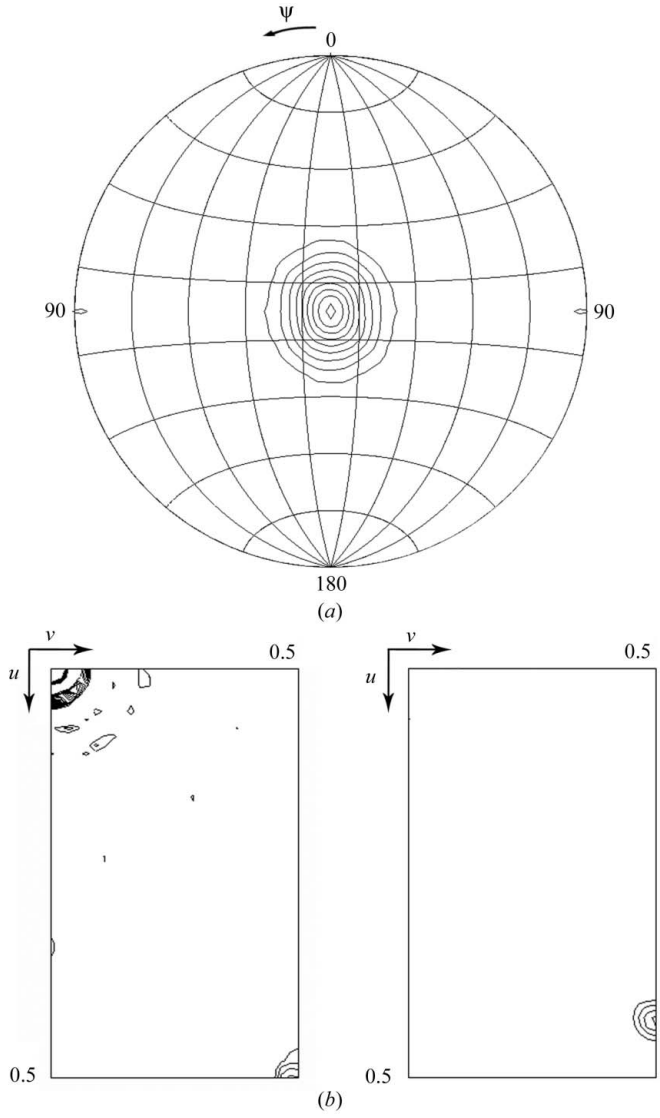

Figure 1
Self-rotation function and native Patterson. (*a*) Self-rotation function calculated using *CNS* (Brünger *et al.*, 1998) in the resolution range 15–4.5 Å, integration radius 5–39 Å. Section at $\kappa = 120^\circ$ showing the threefold peak (9.4σ) aligned with one of the crystallographic 222 axes. Contours start at the 1σ level and increase in 1σ intervals. (*b*) Native Patterson map calculated using the *CCP*4 suite (Collaborative Computational Project, Number 4, 1994) in the resolution range 35–4 Å for a primitive orthorhombic lattice with unit-cell parameters a = 130.1, b = 78.7, c = 171.2 Å. Contours start at 3σ and increase in steps of 2σ. Left, section $w = 0$ showing the origin peak and that at (0.5, 0.49, 0) thought to arise from the pseudo-hexameric symmetry of P2 trimers. Right, section $w = 0.5$. A peak is evident at position (0.43, 0.5, 0.5). Prepared using the program *GROPAT* (R. Esnouf & D. I. Stuart, unpublished program).

Table 1
Native data-collection and processing statistics.

Values in parentheses are for the highest resolution shell 4.31–4 Å.

X-ray source	BM14
Wavelength (Å)	0.99454
Space group	$P2_12_12$
Unit-cell parameters (Å, °)	a = 171.1, b = 78.7, c = 130.1, $\alpha = \beta = \gamma = 90$
Resolution range (Å)	35–4
No. images	305 (1° oscillations)
Observations	358637
Unique reflections	14138
Redundancy	9.1 (8.5)
Completeness (%)	99.1 (98.1)
$I/\sigma(I)$	3.4 (2.4)
$R_{\rm merge}$† (%)	67.8

† $R_{\rm merge} = \sum|I - \langle I\rangle|/\sum\langle I\rangle$.

2.2. Crystallization and data collection

Purified P2 was concentrated at room temperature with a Millipore concentrator (10 kDa molecular-weight cutoff) to ∼2.9 mg ml^{-1}, as measured by the absorbance at 280 nm on a NanoDrop ND-1000 spectrophotometer (NanoDrop Technologies). Crystallization drops were dispensed into a 96-well Greiner plate using a Cartesian robot according to the standard OPPF (Oxford Protein Production Facility) crystallization protocols (Walter *et al.*, 2003, 2005) with a protein: reservoir ratio of 2:1 to a final drop volume of 300 nl. Thin plate-shaped and needle-shaped crystals appeared in several conditions at 298 K almost immediately after setup and reached maximum dimensions after 36–48 h (these conditions tended to contain both polyethylene glycol polymers and monovalent ions at a concentration of around 200 m*M*). Crystallization was monitored by automatic imaging (Mayo *et al.*, 2005). Prior to crystal optimization, a crystal was selected from the screen for diffraction analysis. The crystal used grew to approximate dimensions of 0.17 × 0.03 × 0.005 mm in the presence of 22.5%(*w*/*v*) PEG smear, 100 m*M* Bis-Tris propane pH 6.5 and 200 m*M* sodium iodide. The PEG smear is a mixture of ten polyethylene glycol polymers of various molecular weights ranging from 200 to 10 000 (molecular weights of 200, 400, 600, 1000, 1500, 3000, 4000, 6000, 8000 and 10 000, introduced by Janet Newman; manuscript in preparation). Diffraction data from this first crystal were collected at beamline BM14, ESRF and measured on a MAR Mosaic 225 CCD detector (a 100 µm beam aperture was used). Because of the extreme thinness of the crystals and the small drop volume, particular care was required in transferring the crystals for a few seconds into PFO-125/03 (perfluoropolyether) cryoprotectant oil prior to flash-freezing in a nitrogen-gas stream. Data were processed and indexed using *HKL*2000 (Otwinowski & Minor, 1997); statistics are shown in Table 1. Even though the data are extremely weak owing

to the tiny volume of crystal irradiated, the statistics are nonetheless roughly in line with what would be expected on the basis of counting statistics and the data are sufficiently rich in information to reveal the organization of the molecules within the crystal.

3. X-ray data analysis

The data set was initially autoindexed in a primitive orthorhombic lattice, with unit-cell parameters $a = 130.1$, $b = 78.7$, $c = 171.2$ Å. The overall weakness of the data and the paucity of reflections corresponding to potential systematic absences made the identification of twofold screw axes ambiguous at this stage. The self-rotation function for these data was calculated using *CNS* (Brünger *et al.*, 1998) and showed the presence of a peak at $\psi = 0, \varphi = 0, \kappa = 120^\circ$ corresponding to a non-crystallographic threefold axis aligned along the *c* axis in the above indexing scheme (Fig. 1*a*). The unit-cell volume is sufficient to contain two trimers per asymmetric unit and 47% solvent by volume. A native Patterson function calculated at 4 Å resolution revealed two unique peaks of similar height [(0.43, 0.5, 0.5) and (0.5, 0.49, 0); Fig. 1*b*]. Analysis of the relative peak heights in Patterson maps calculated over a number of different resolution ranges suggests that the vector (0.43, 0.5, 0.5) is that most likely to relate two similarly oriented trimers in the asymmetric unit. Note that this peak is sufficiently displaced from (0.5, 0.5, 0.5) that even at low resolution we do not observe pseudo-*I*-centring.

Next, a pseudo-atom P2 model derived from the 7 Å resolution X-ray electron-density map of the entire PM2 bacteriophage (Abrescia *et al.*, unpublished results) was orientated to align the molecular threefold axis with the self-rotation peak and the residual rotational ambiguity was resolved by monitoring the correlation coefficient (CC) in E^2 during a systematic rotation about this axis (performed in space group *P*1 with the two trimers locked to have the translational relationship defined above) using the program *X-PLOR* (Brünger, 1992). Finally, the identification of the correct space group and the determination of the position of the molecules with respect to the crystallographic axes was achieved using *X-PLOR* by systematically monitoring the CC during PC refinement (Brünger, 1992) followed by translation searches (CC in E^2 target function; 20–8 Å resolution) in all possible space groups for point group 222 including the non-standard space groups such as $P2_122_1$ and $P22_12_1$. $P22_12_1$ gave the highest CC (45.8%) and good packing with few molecular collisions (Fig. 2). In this arrangement, the trimers pack closely side by side, forming a series of infinite stacked planes, with their non-crystallographic threefold axes arranged perpendicular to the planes. The proliferation of side-to-side P2 interactions favours lateral crystal growth, reflecting the plate-like crystal morphology. Interestingly, this packing appears to recapitulate some of the molecular interactions seen in the virus capsid, an effect previously reported for African horse sickness virus (AHSV; Basak *et al.*, 1996). However, whilst the arrangement of trimeric coat proteins in viruses of the PRD1-adenovirus lineage has local *p*3 symmetry (Abrescia *et al.*, 2004), adjacent rows of trimers in Fig. 2 are rotated by 60° with respect to each other. We note that the trimeric molecules possess pseudo-sixfold symmetry (Huiskonen *et al.*, 2004; Abrescia *et al.*, unpublished results) which introduces a pseudo-non-crystallographic translation between the non-crystallographically related trimers within the plane (Fig. 2). This corresponds to the second peak in the native Patterson map (0.5, 0.49, 0). At the present stage in the analysis, we cannot entirely rule out the possibility that this second peak corresponds to a genuine non-crystallographic translation, in which case the first peak would arise from a pseudo-non-crystallographic translation. We intend to resolve this ambiguity and determine the atomic structure of P2 by SeMet labelling and phase determination by MAD phasing, if necessary using phase information derived from the low-resolution viral P2 pseudo-atomic model to assist the process.

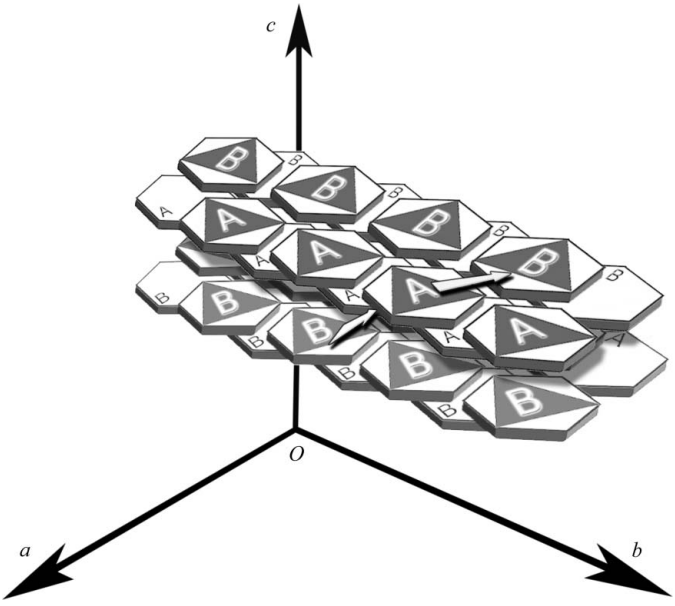

Figure 2
Cartoon representation of trimer packing. The hexameric morphology of the P2 trimers is denoted by solid hexagons, while their underlying trimeric nature and orientation is denoted by black triangles. *A* and *B* label the two crystallographically independent trimers, which by application of crystallographic symmetry form a series of infinite and closely spaced planes. The lower left arrow corresponds to the Patterson vector (0.43, 0.5, 0.5), while the arrow at the upper right corresponds to the Patterson vector (0.5, 0.49, 0) and relates (by a 60° rotation) *A* and *B* trimers in the same plane.

We are grateful to P. Papponen for excellent technical assistance in virus production and protein purification, to M. Bahar for help with synchrotron data collection and T. Walter for advice with the Cartesian robot. The authors thank the staff at the UK beamline BM14, ESRF, Grenoble. BM14 is supported by the UK Research Councils, the BBSRC, the EPSRC and the MRC. The OPPF is supported by the Medical Research Council, UK. The work was supported by the Human Frontier Science Project (RGP0320/2001-M), the Academy of Finland grants 1201964 (JKHB) and 1202108 (DHB), the Finnish Centres of Excellence Program 2000–2005 (1202855), the EU (SPINE-QLG2-CT-2002-00988) and the Medical Research Council, UK. JMG is supported by the Royal Society and DIS by the Medical Research Council, UK.

References

Abrescia, N. G., Cockburn, J. J., Grimes, J. M., Sutton, G. C., Diprose, J. M., Butcher, S. J., Fuller, S. D., San Martin, C., Burnett, R. M., Stuart, D. I., Bamford, D. H. & Bamford, J. K. (2004). *Nature (London)*, **432**, 68–74.
Bamford, D. H., Burnett, R. M. & Stuart, D. I. (2002). *Theor. Popul. Biol.* **61**, 461–470.
Bamford, D. H. (2003). *Res. Microbiol.* **154**, 231–236.
Basak, A. K., Gouet, P., Grimes, J., Roy, P. & Stuart, D. (1996). *J. Virol.* **70**, 3797–3806.
Benson, S. D., Bamford, J. K., Bamford, D. H. & Burnett, R. M. (2004). *Mol. Cell*, **16**, 673–685.
Brünger, A. T. (1992). *X-PLOR, Version* 3.1. *A System for X-ray Crystallography and NMR*. New Haven, CT, USA: Yale University Press.
Brünger, A. T., Adams, P. D., Clore, G. M., DeLano, W. L., Gros, P., Grosse-Kunstleve, R. W., Jiang, J.-S., Kuszewski, J., Nilges, M., Pannu, N. S., Read,

R. J., Rice, L. M., Simonson, T. & Warren, G. L. (1998). *Acta Cryst.* D**54**, 905–921.
Büchen-Osmond, C. (2003). *ICTVdB – The Universal Virus Database*, v.3. http://www.ncbi.nlm.nih.gov/ICTVdb/ICTVdB/.
Cockburn, J. J., Abrescia, N. G., Grimes, J. M., Sutton, G. C., Diprose, J. M., Benevides, J. M., Thomas, G. J. Jr, Bamford, J. K., Bamford, D. H. & Stuart, D. I. (2004). *Nature (London)*, **432**, 122–125.
Collaborative Computational Project, Number 4 (1994). *Acta Cryst.* D**50**, 760–763.
Espejo, R. T. & Canelo, E. S. (1968*a*). *Virology*, **34**, 738–747.
Espejo, R. T. & Canelo, E. S. (1968*b*). *J. Bacteriol.* **95**, 1887–1891.
Harrison, S. C., Caspar, D. L., Camerini-Otero, R. D. & Franklin, R. M. (1971). *Nat. New Biol.* **229**, 197–201.
Huiskonen, J. T., Kivela, H. M., Bamford, D. H. & Butcher, S. J. (2004). *Nature Struct. Mol. Biol.* **11**, 850–856.
Kivelä, H. M., Kalkkinen, N. & Bamford, D. H. (2002). *J. Virol.* **76**, 8169–8178.
Kivelä, H. M., Männistö, R. H., Kalkkinen, N. & Bamford, D. H. (1999). *Virology*, **262**, 364–374.
Männistö, R. H., Kivelä, H. M., Paulin, L., BAmford, D. H. & Bamford, J. K. H. (1999). *Virology*, **262**, 355–363.
Mayo, C. J., Diprose, J. M., Walter, T. S., Berry, I. M., Wilson, J., Owens, R. J., Jones, E. Y., Harlos, K., Stuart, D. I. & Esnouf, R. M. (2005). *Structure*, **13**, 175–182.
Nandhagopal, N., Simpson, A. A., Guron, J. R., Yan, X., Baker, T. S., Graves, M. V., Van Etten, J. L. & Rossmann, M. G. (2002). *Proc. Natl Acad. Sci. USA*, **99**, 1458–14763.
Otwinowski, Z. & Minor, W. (1997). *Methods Enzymol.* **276**, 307–326.
Walter, T. S., Diprose, J., Brown, J., Pickford, M., Owens, R. J., Stuart, D. I. & Harlos, K. (2003). *J. Appl. Cryst.* **36**, 308–314.
Walter, T. S., Diprose, J. M., Mayo, C. J., Siebold, C., Pickford, M. G., Carter, L., Sutton, G. C., Berrow, N. S., Brown, J., Berry, I. M., Stewart-Jones, G. B. E., Grimes, J. M., Stammers, D. K., Esnouf, R. M., Jones, E. Y., Owens, R. J., Stuart, D. I. & Harlos, K. (2005). *Acta Cryst.* D**61**, 651–657.